

Fullerene Dimers (C₆₀/C₇₀) for Energy Harvesting

Juan L. Delgado,^[a, b] Eva Espíldora,^[a] Moritz Liedtke,^[c] Andreas Sperlich,^[d]
Daniel Rauh,^[c] Andreas Baumann,^[d] Carsten Deibel,^[d] Vladimir Dyakonov,^{*,[c, d]} and
Nazario Martín^{*,[a, b]}

Abstract: A new family of fullerene-based compounds, namely, soluble [60]- and [70]fullerene homodimers and the [60]/[70]heterodimer linked through 2-pyrazolino-pyrrolidino bridges, has been synthesised by simple procedures and in high yield. Electrochemical studies confirm their suitability to act as electron acceptors in combination with poly(3-hexylthiophene-2,5-diyl) (P3HT). Their optical properties in solution and in the solid state were studied. A significantly stronger absorption

in [70]fullerene-containing dimers relative to [60]homodimer in solution in the visible range was observed. Furthermore, in all donor-acceptor blends studied an efficient charge transfer was observed by means of photoluminescence (PL), photoinduced absorption and light-induced electron spin reso-

nance spectroscopy. The [70]homodimer was found to be a distinctive species, being the strongest PL quencher and most efficient acceptor with the longest lifetime of the charge-separated (polaron) states. As a consequence, bulk-heterojunction solar cells based on this novel [70]homodimer blended with P3HT demonstrated the highest quantum and power conversion efficiencies of 37 and 1%, respectively, compared to those of [60]fullerene dimers.

Keywords: charge transfer • dimerization • energy conversion • EPR spectroscopy • fullerenes

Introduction

Global dependence on fossil fuels is a key issue with important consequences in the world nowadays.^[1] A reasonable alternative to overcome this need is the use of renewable energy sources,^[2] such as solar energy, which could, in principle, fulfil our energy requirements with environmentally clean procedures and low prices.

In this context, the development of photovoltaic (PV) devices based on organic materials, suitable for converting solar energy into electrical power, is currently a challenging matter. The mostly efficient organic solar cells to date show efficiencies in the range of 5–6%^[3] and are based on phase-separated polymer-fullerene blends with donor-acceptor properties. In such blends, fullerenes and their derivatives possess important properties, such as small reorganisation energy, high electron affinity, ability to transport charge and stability, which makes them the best candidates to act as electron-acceptor components in bulk-heterojunction (BHJ) PV devices.^[4,5] Typical conjugated-polymer donor counterparts are poly(3-hexylthiophene-2,5-diyl) (P3HT), poly[2-methoxy-5-(3',7'-dimethyloctyloxy)]-1,4-phenylenevinylene (MDMO-PPV) and polyfluorenes as well as their copolymers.^[6] Compared with the great variety of conjugated polymers tested, only a few structurally different fullerene deriv-

[a] Dr. J. L. Delgado, Dr. E. Espíldora, Prof. Dr. N. Martín
Departamento de Química Orgánica, Facultad de Ciencias Químicas
Universidad Complutense de Madrid
28040 Madrid (Spain)
Fax: (+34) 913-944-103
E-mail: nazmar@quim.ucm.es

[b] Dr. J. L. Delgado, Prof. Dr. N. Martín
IMDEA-Nanociencia, Facultad de Ciencias
Ciudad Universitaria de Cantoblanco
28049 Madrid (Spain)

[c] M. Liedtke, D. Rauh, Prof. Dr. V. Dyakonov
Bavarian Centre for Applied Energy Research (ZAE Bayern)
Am Hubland, 97074 Würzburg (Germany)

[d] A. Sperlich, A. Baumann, Dr. C. Deibel, Prof. Dr. V. Dyakonov
Experimental Physics VI
Julius-Maximilians-University of Würzburg
Am Hubland, 97074 Würzburg (Germany)
Fax: (+49) 931-31-83109
E-mail: dyakonov@physik.uni-wuerzburg.de

Supporting information for this article is available on the WWW under <http://dx.doi.org/10.1002/chem.200902039>. It contains synthetic procedures, characterisation details for the new compounds, additional electron spin resonance data and PL results concerning the effect of thermal treatment of the blend films.

atives have been synthesised and used in the preparation of BHJ-PV devices so far.^[7] To date, [6,6]-phenyl C₆₁ butyric acid methyl ester (PCBM), first synthesised by Hummelen and Wudl in 1995,^[8] remains the fullerene derivative most employed in the preparation of BHJ-PV devices. Based on this methanofullerene, which has been intensively studied worldwide for more than a decade, reproducible power conversion efficiencies (PCEs) in the range of 5% under air mass 1.5 (AM1.5) conditions at 100 mW cm⁻² have been reported.^[9]

Belonging to the same class of methanofullerenes, 1,1-bis(4,4'-dodecyloxyphenyl)-(5,6) C₆₁, diphenylmethanofullerene (DPM-12) was another acceptor system showing a promising PCE of 2.3%.^[10] A recently reported naphthalene-fused fullerene derivative has been proved to show performances (4.5%) similar to those achieved with PCBM.^[11] Interestingly, it has recently been found that fullerene derivatives with more negative reduction potentials (poorer electron acceptors) than the parent PCBM give rise to higher values of the open-circuit voltage (V_{OC}), thus resulting in higher efficiencies in the PV device.^[12]

Among other parameters, the ability of the conjugated polymer and the fullerene derivative to harvest sunlight is essential to obtain a good performance of the PV device. However, [60]fullerene derivatives display a low absorption in the visible region, due to the high degree of symmetry (I_h) of the molecule, thus limiting the utilisation of solar light in the BHJ-PV device. Therefore, the search for new fullerene-based materials able to collect sunlight more efficiently remains an important challenge to be addressed. [70]PCBM came into play recently due to its improved optical absorption.^[13] Stimulated by the idea of combining good electron-accepting and light-harvesting properties, we now introduce a new class of fullerene-based materials constituted by two covalently connected fullerene units (C₆₀ and/or C₇₀). The resulting dimers, endowed with a solubilising alkyl chain, exhibit increased light-harvesting properties due to the presence of two units of identical (**4**, **6**) or different (**5**) fullerenes linked through a 2-pyrazoline moiety and a pyrrolidine ring (Figure 1).

A variety of [60]fullerene dimers bearing different connecting bridges have been described so far.^[14] However, the preparation of [60]/[70]fullerene heterodimers and

[70]fullerene homodimers remains a much less explored field. Furthermore, the fullerene dimers are known to exhibit poor solubility in common organic solvents, which has prevented their use in optoelectronic devices to a great extent.^[14] Their PV applications are, however, of interest because they are expected to improve the molar absorptivity, due to the presence of two fullerenes and/or to the better light-absorbing properties of C₇₀ relative to C₆₀. Herein, we report the electrochemical and photophysical properties of these new homo- (**4**: C₆₀-C₆₀; **6**: C₇₀-C₇₀) and heterodimers (**5**: C₆₀-C₇₀) as well as of their blends with P3HT. We established excellent film-forming properties for all blends due to the high solubility of the dimers in common organic solvents. Photoinduced electron transfer was found to occur in all BHJs studied and was most efficient in P3HT/C₇₀-C₇₀. Preliminary tests of BHJ-PV devices built with C₇₀-C₇₀/P3HT blends demonstrated an external quantum efficiency (EQE) of 37% as well as non-optimised PCE in the range of 1%. All three types of solar cells show a short-circuit current density of 5, 4.3 and 3.4 mA cm⁻² for P3HT/C₇₀-C₇₀, P3HT/C₆₀-C₆₀ and P3HT/C₆₀-C₇₀, respectively. The reduced PV performance of the heterodimer can be explained by inefficient exciton dissociation in the BHJ. Finally, we provide the first experimental identification of the negative polarons (radical anions) localised on C₇₀-C₇₀ and C₆₀-C₇₀ dimer cages in the P3HT composites by using a light-induced electron spin resonance (LESR) technique. Interestingly, in C₆₀-C₇₀ dimers we were able to distinguish between electrons on the C₆₀ cage and the C₇₀ cage. This opens up a completely new possibility to study electron-electron interactions in well-defined molecular systems.

Results and Discussion

Synthesis: The preparation of C₆₀-containing dimers **4** and **5** was carried out in a single step, starting from our recently described formyl-containing building block (**7**) (Scheme 1).^[15] This aldehyde was reacted with *N*-octylglycine and an excess of [60]- and [70]fullerene to prevent the intramolecular cycloaddition of the in situ generated azomethyne ylide on the fullerene sphere in **7**. The respective dimers were obtained in high yields and easily isolated by column chromatography due to their high solubility in carbon disulfide. The structure and purity of each compound were confirmed by different spectroscopic techniques, which allowed detection of a mixture of isomers for heterodimer **5**, as well as a small amount of **4** resulting from the low C₆₀ impurity concentration in the commercial C₇₀ used for the synthesis. Monofunctionalisation of C₇₀ preferentially

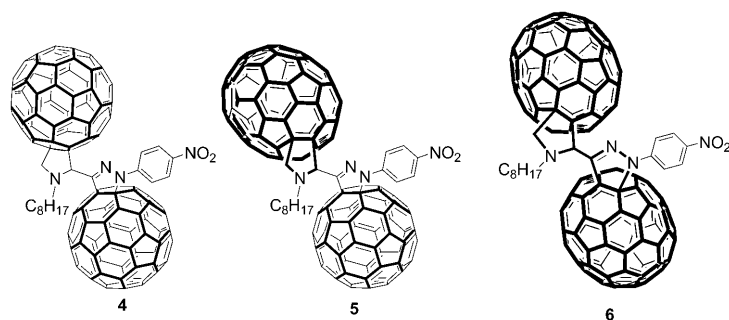
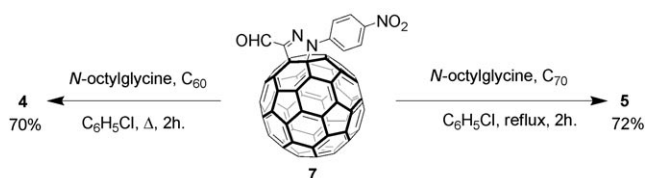


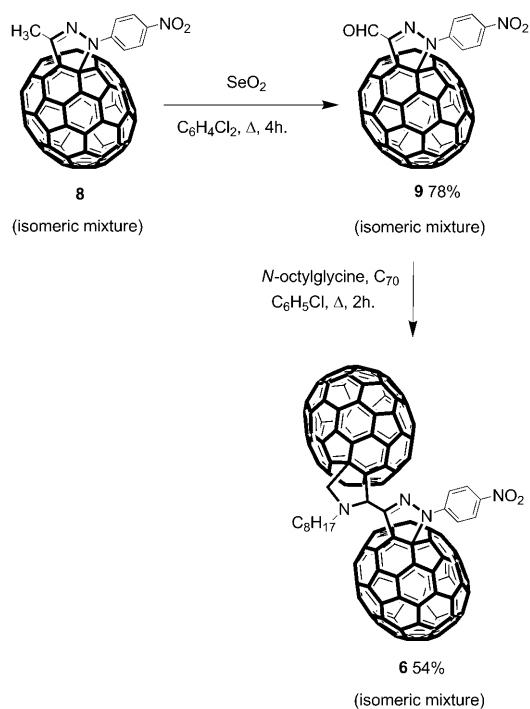
Figure 1. [60]- and [70]fullerene homodimers (**4**, **6**) and heterodimer (**5**). Dimers **5** and **6** are obtained as a mixture of isomers.



Scheme 1. Synthesis of dimer compounds **4** and **5**.

yields C(1)–C(2) (type α) adducts,^[16] with the C(5)–C(6) (type β) adduct being the second most favoured compound. In the case of 1,3-cycloaddition of azomethine ylides to C_{70} , the addition of the dipole to the C(7)–C(21) bond also takes place as a less-favoured process.^[17] Therefore, considering our C_s -symmetrical azomethine ylide, six possible isomers can be generated through the reaction of the dipole with C_{70} . Indeed, compound **5** is obtained as a mixture of isomers as observed by $^1\text{H NMR}$ spectroscopy (see the Supporting Information); four isomers are formed in different proportions (39, 30, 22 and 9% by $^1\text{H NMR}$) together with a small quantity of compound **4** (3% by HPLC), due to the above-mentioned presence of C_{60} in the commercial C_{70} . To date only a small number of C_{60} – C_{70} heterodimers have been described,^[18] some of them prepared by a mechanochemical solid-state reaction.^[19] Furthermore, their low solubility in common organic solvents has usually prevented their use in further applications. In our case, the presence of the octyl chain on the pyrrolidine nitrogen atom in **4**–**6** allowed us to obtain stable solutions of the dimers in organic solvents and, consequently, facilitate their characterisation as well as their incorporation into BHJ-PV devices.

The synthesis of C_{70} homodimer **6** was accomplished in a two-step procedure from derivative **8**,^[20] which was oxidised with selenium dioxide according to our previously described methodology^[15] to afford the new aldehyde **9** in very good yield (78%). This formyl-bearing [70]fullerene was then reacted following the methodology of Prato et al.^[21] in the presence of *N*-octylglycine and an excess of [70]fullerene to afford compound **6** in a relatively good yield (52%; Scheme 2). Dimer **6** is formed of a mixture of isomers, the composition of which was studied by high-pressure liquid chromatography (HPLC). Interestingly, precursor **9** is formed by three aldehyde- C_{70} isomers (**9a**: 32%, **9b**: 38%, **9c**: 30% by $^1\text{H NMR}$)^[22] and a small amount of **7** resulting from the C_{70} sample used, which contains around 2% of pristine C_{60} (MER Corporation). When this mixture is reacted with *N*-octylglycine and C_{70} , 18 possible C_{70} – C_{70} isomers can be formed in addition to six possible C_{60} – C_{70} isomers, as well as three additional C_{70} – C_{60} dimers, very small amounts of which can be formed, if any. This complex isomeric mixture was detected by HPLC (toluene, 1 mL min^{-1}) and assigned by studying its UV/Vis spectra, although it was not possible to isolate the components by using chromatographic techniques. Therefore, dimer **6** as a mixture of C_{70} – C_{70} (96% by HPLC) and C_{70} – C_{60} / C_{60} – C_{70} isomers (4% by HPLC; see the Supporting Information) was used in these studies.



Scheme 2. Synthesis of dimer compound **6**.

It is worth mentioning that in the above search for new materials, this new family of compounds represents the first example of covalently bonded pyrrolidino-pyrazolino-fullerene dimers. Although both fullerene families, pyrrolidinofullerenes^[21] and pyrazolinofullerenes,^[23] are well known in fullerene chemistry and have been extensively studied, to the best of our knowledge this is the first report on molecules containing both organic fragments and, therefore, their properties and applications are still unexplored.

Optical properties: Bridging two fullerenes together may have several consequences for the photophysics of the polymer–dimer blends. They are of intrinsic nature, for example due to enhanced molecular absorptivity of C_{70} -based dimers, but are also extrinsic by influencing the blend morphology. The optical absorption spectra of compounds **4**–**6** in toluene solution are shown in Figure 2. Compound **4** displays a typical [60]fullerene derivative absorption pattern, showing weak absorption in the visible region. In the UV region, the values of molar absorptivity for this dimer (**4**) are larger by approximately a factor of 2 than those observed for precursor **7**. In the case of heterodimer **5**, characteristic bands for both [60]fullerene precursor **7** (287, 325 nm) and [70]fullerene (397, 468, 544 nm) are observed, which comprise a superimposition of two components. For the [70]homodimer **6**, representative absorption features of [70]fullerenes are seen. Moreover, as can be seen in Figure 2, the molar absorptivity values for these bands are approximately double that observed for compound **5**, which contains one [70]fullerene unit only. As a consequence of the [70]fullerene-related optical absorption in the visible range, solutions of compound

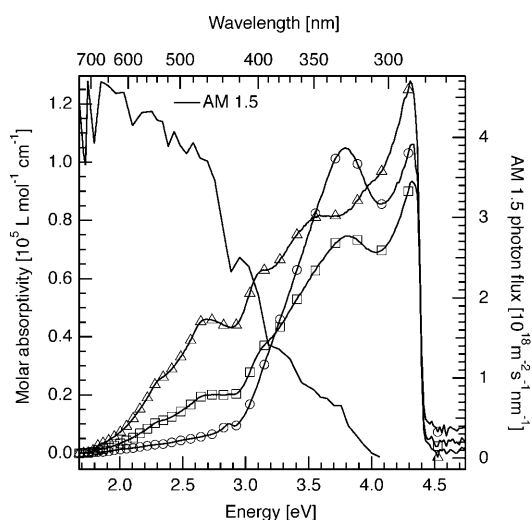


Figure 2. Molar absorption coefficient spectra for dimers **4** (○), **5** (□) and **6** (△) in toluene solution at 1×10^{-5} M.

5 display a characteristic red-brown colour, which is even darker for the dimer **6** (see the Supporting Information). The observed enhancement in the absorption from **4** to **6** is a consequence of the presence of the [70]fullerene unit and may become very important for improving the efficiency of PV devices.

UV/Vis absorption spectra of solid blends are shown in Figure 3. The **4–6** dimers blended with P3HT (1:1 ratio) have in general the same spectral features as P3HT/[60]PCBM blend. On the other hand, the absorption curves for new dimer blends are redshifted by 25 nm with respect to P3HT/[60]PCBM. The observed shift may result not only from the carbon chains bridging the two fullerene molecules, but also from the effect of better crystallisation of P3HT in

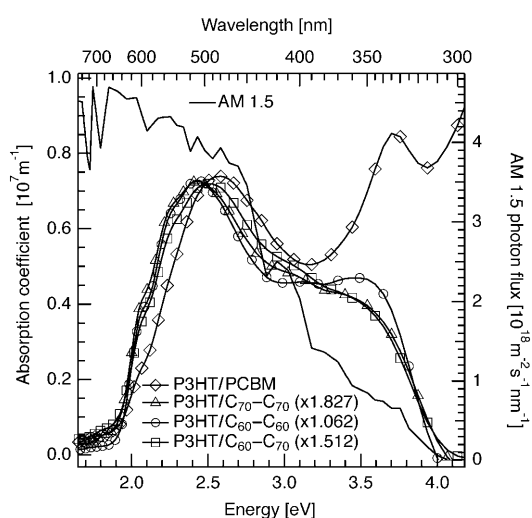


Figure 3. Absorption coefficients of blends of the fullerene dimers **4–6** with P3HT as indicated in the legend. The AM1.5 solar spectrum and the absorption of P3HT/[60]PCBM are shown for reference. All coefficients are normalised to that of P3HT/[60]PCBM at 500 nm; the normalisation factors are given in parentheses.

combination with our novel dimers. Note that the absorption spectra of P3HT and [70]fullerenes in the visible range are strongly overlapping.

Photoluminescence (PL) measurements performed on the same systems in the solid state are shown in Figure 4. PL originates from the radiative recombination of singlet exci-

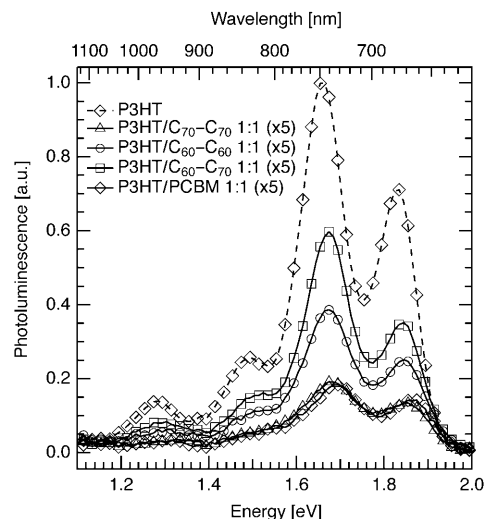


Figure 4. PL of blends of P3HT and fullerene dimers **4–6**, magnified by a factor of 5, in comparison to the PL of pristine P3HT (----) at $T=30$ K. Excitation was with a 514 nm laser. The weak PL signal of P3HT/C₇₀-C₇₀ indicates an efficient charge-carrier separation comparable to that of P3HT/[60]PCBM.

tions formed on P3HT chains. Laser light of wavelength 514 nm was used for the initial singlet excitation. The PL quenching may be due to the following effects: 1) photoinduced charge transfer between polymer and fullerene; 2) resonance energy transfer between species in the excited and ground states due to overlap of emission and absorption spectra; and iii) structural modification upon blending and thermal treatment of the sample, which affects the self-quenching of the initial excitation (see the Supporting Information). For the occurrence of charge transfer, the binding energy of the photogenerated exciton corrected for Coulomb attraction between separated charges should be smaller than the difference in the electron affinities of the participating donor and acceptor species. The PL studies alone are not sufficient to justify one or another process. Strong PL quenching may, however, serve as an indicator for charge-carrier transfer between donor and acceptor in blends, for which additional experiments are needed. According to cyclic voltammetry (CV) studies (see below), electron transfer between P3HT and dimers **4–6** is energetically possible. As follows from Figure 4, the PL quenching is observed in all compounds; however, only the [70]homodimer quenches the luminescence in P3HT as strongly as [60]PCBM. We also note the same vibronic structure of the residual PL in the blends, which is a sign of no additional interaction influencing the elementary excitation process. The difference in

PL quenching for different dimers is quite obvious. The strongest residual PL (the weakest quenching) is found in the P3HT/C₆₀-C₇₀ sample. As we shall see later, this is reflected in the charge-generation efficiency and may be due to different phase separation (demixing) in the studied films.

Electrochemistry: The redox behaviour of dimers **4–6** was studied by Osteryoung square-wave voltammetry (OSWV), as shown in Figure 5. It is mainly characterised by the ap-

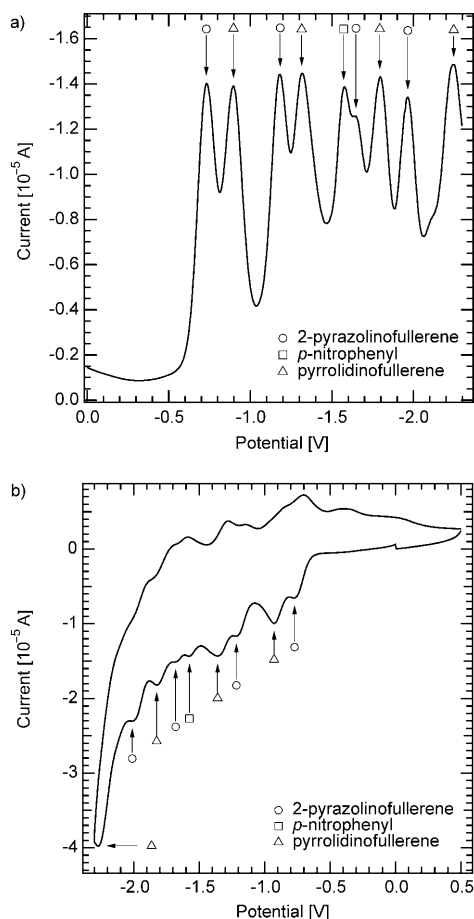


Figure 5. a) OSWV of dimer **4** in *o*-dichlorobenzene/acetonitrile (ODCB/MeCN, 4:1). b) Cyclic voltammogram of dimer **4** with reduction waves as indicated.

pearance of two sets of reduction waves owing to the presence of two distinct pyrrolidino- and 2-pyrazolinofullerene units. The [60]- or [70]-2-pyrazolinofullerene moieties display quasi-reversible reduction waves with potentials 50–70 mV, that is, more positive than those of the parent C₇₀ or C₆₀ due to the electron-withdrawing effect of the pyrazoline ring.^[20] In contrast, [60]- or [70]pyrrolidino fragments show reduction potentials shifted to more negative values compared to those of the parent fullerenes, as a consequence of the saturation of a double bond on the fullerene sphere, which raises the LUMO energy level (Table 1).^[24] Compounds **4–6** and aldehydes **7** and **9** displayed additional non-reversible CV waves around 1.63–1.65 V corresponding to

Table 1. Redox potentials (OSWV) of dimers **4–6**, aldehydes **7** and **9**, C₆₀ and C₇₀.^[a]

Compound	E^1_{red}	E^2_{red}	E^3_{red}	E^4_{red}
4	-0.72	-0.90	-1.17	-1.32
5	-0.73	-0.90	-1.16	-1.31
6	-0.72	-0.87	-1.14	-1.30
7	-0.75	-1.15	-1.61	-2.06
9	-0.75	-1.11	-1.56	-1.91
C ₆₀	-0.78	-1.19	-1.66	-2.11
C ₇₀	-0.77	-1.15	-1.56	-1.97

[a] V vs. Ag/AgNO₃; glassy carbon electrode as the working electrode; 0.1 M Bu₄N⁺PF₆⁻; ODCB/MeCN (4:1); scan rate = 100 mV s⁻¹.

the reduction of the *p*-nitrophenyl moiety, which is consistent with related systems.^[23d]

Comparison of the first reduction potentials of dimers **4** and **5** and aldehyde **7** reveals the existence of a weak electronic interaction in the ground state. Thus, when the formyl group is replaced by the pyrrolidinofullerene moiety, the first reduction potential of the 2-pyrazolinofullerene unit is shifted by 20 to 30 mV to more positive values. A similar behaviour is observed for dimer **6**, which shows reduction potentials 30 mV more positive than that observed for **9** which bears a formyl substituent. Nevertheless, according to the observed data, we can conclude that both 2-pyrazolinofullerene and pyrrolidinofullerene behave almost independently in the ground state.

Photoinduced absorption: Quasi-steady-state photoinduced absorption (PIA) is a method to probe long-living excited states in conjugated polymers and their blends.^[25] In pure P3HT, the singlet excitons are clearly seen as a dominant peak at 1.03 eV (Figure 6).^[26] Once blended with a strong

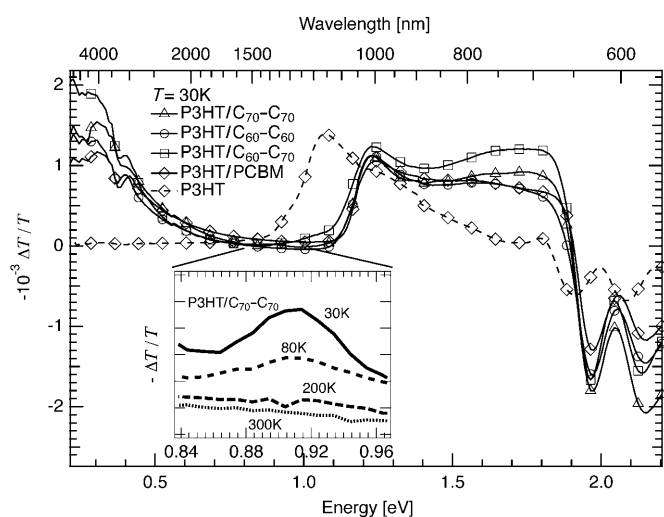


Figure 6. PIA signals of the homo- and heterodimers blended with P3HT, as indicated in the legend. The low-energy and high-energy polaron signals at 0.3 and 1.2 eV, respectively, are seen in the blends P3HT/dimers **4–6**. Inset: Temperature dependences of PIA peaks in C₇₀-C₇₀/P3HT blend. The 0.9 eV peak—negative polaron on C₇₀ homodimer—is visible only at low temperatures.

electron acceptor, for example [60]PCBM, absorption bands of radical cations (positive polarons) can be seen in the PIA spectrum at 0.3 and 1.2 eV corresponding to low- and high-energy peaks, respectively. The PIA spectra for P3HT blended with dimers **4–6** are shown in Figure 6. In all three blends, the 0.3 and 1.2 eV polaron peaks are present. The spectrum of P3HT/C₆₀–C₆₀ looks nearly identical to that of P3HT/PCBM. In contrast, P3HT/C₇₀–C₇₀ reveals an additional PIA peak at 0.9 eV, which is strongly temperature dependent (see inset to Figure 6) and can only be detected at low temperatures. Its origin is unknown and will be discussed later. In P3HT/C₆₀–C₇₀, a shoulder at 1.03 eV shows up. Taking the PIA spectrum of the pure P3HT into account, we conclude that the shoulder at 1.03 eV may be due to either incomplete dissociation of singlet excitons at low temperatures, or to other excited states. Possible candidates are triplet excitons and/or charge-transfer excitons, also called polaron pairs. To be consistent with the observation of a stronger PL found in the same dimer blends, the recombination of these excited states should lead to the formation of singlet excitons and thus to a stronger PL in C₆₀–C₇₀ (see Figure 4). Furthermore, the lifetime of singlet excitons, triplet excitons and polaron pairs is expected to be very different.

To investigate these new PIA peaks in more detail, frequency-dependent PIA measurements were performed. The modulation (on–off) frequency of the excitation laser light was varied in a broad frequency range. The PIA response R on the modulated excitation was described as suggested by Epshtein et al. [Eq. (1)]:^[27]

$$R = \frac{R(\omega = 0)}{1 + (i\omega\tau)^\alpha} \quad (1)$$

where ω is the modulation (chopper) frequency, $R(\omega=0)$ is the PIA signal at $\omega=0$, τ is the effective (mean) lifetime, i is the imaginary unit, and α is a constant indicating the dominant recombination process, with $\alpha=1$ indicating pure monomolecular recombination. We fitted the experimental data with Equation (1), and the parameters α and τ for the polaron peaks at 0.3 and 1.2 eV and for the yet unidentified peaks at 1.03 and 0.9 eV are summarised in Table 2. (Due to a strong temperature dependence of the PIA signals at 0.9 and 1.03 eV, measurements were not possible at 200 K and at room temperature.) All PIA bands respond on the modulation frequency with a fractional power law dependence with α between 0.59 and 0.79, and nearly a constant at low temperatures. The α values for the 1.03 eV peak in the

Table 2. PIA lifetimes and α factors for three P3HT/dimer blends for the different excited states at $T=30, 80, 200$ K and room temperature. All PIA bands, except that at 1.03 eV in P3HT/C₆₀–C₇₀, show the same trend of decreasing τ and α with increasing temperature. The 1.03 eV state in P3HT/C₆₀–C₇₀ shows a temperature-independent α . $\Delta\alpha$ is ± 0.01 for all values.

Blends	T Peaks [eV]	30 K		80 K		200 K		RT	
		τ [μ s]	α						
P3HT/C ₆₀ –C ₆₀	1.23	89	0.72	59	0.69	9	0.70	1	0.59
	0.30	94	0.72	63	0.69	8	0.79	2	0.58
P3HT/C ₆₀ –C ₇₀	1.23	74	0.73	54	0.72	9	0.77	2	0.68
	1.03	56	0.69	58	0.69				
P3HT/C ₇₀ –C ₇₀	0.30	80	0.73	54	0.72	9	0.78	2	0.70
	1.23	110	0.71	85	0.69	27	0.63	9	0.61
	0.90	117	0.72	77	0.71				
	1.21	117	0.71	80	0.69	27	0.63	10	0.60
P3HT/PCBM	1.23	85	0.80	41	0.76	7	0.80	2	0.69
	0.30	187	0.80	41	0.77	8	0.85	6	0.34

P3HT/C₆₀–C₇₀ blend are lower than those for other peaks. The effective lifetime τ of polaron states (0.3 and 1.2 eV) strongly decreases from 90 μ s ($T=30$ K) to 1 μ s (room temperature). The same holds true for the PIA band at 0.9 eV, whereas the lifetime of the exciton peak at 1.03 eV (around 60 μ s) is unaffected by temperature. Interestingly, in the whole temperature range available, the excited states in P3HT/C₇₀–C₇₀ blends have the longest lifetimes relative to other dimer blends. The assignment of PIA absorption bands at 0.9 and 1.03 eV to particular states, polarons, polaron pairs and singlet (or triplet) excitons is not completely reliable. According to the long lifetime, the singlet exciton origin of the 1.03 eV peak can be excluded. Instead, the triplet exciton and charge-transfer exciton scenarios should be further assessed. To identify them unambiguously, spin-sensitive techniques will be necessary, which are presented in the following section.

Electron spin resonance: ESR measurements on pure P3HT and on pure fullerene dimers in the dark and under illumination show no signal except for compound **4**. In the latter, a small light-induced signal of the C₆₀-related radical anion was detected (not shown), which indicates the presence of minor impurities.

The ESR signals (Figure 7) found in the 1:1 blends of P3HT/[60]PCBM and in P3HT blended with compound **4** (C₆₀–C₆₀) show nearly the same signal shape and g values, which is a sign of efficient electron transfer between P3HT and the C₆₀–C₆₀ dimer. Although the ESR spectrum of blends of P3HT and heterodimers C₆₀–C₇₀ shows nearly the same spectral shape as those for P3HT/C₆₀–C₆₀ and P3HT/[60]PCBM, the ESR peak corresponding to the C₆₀ radical anion is significantly smaller than the radical cation peak (P3HT peak). Even more dramatic is the modification of the ESR spectrum in the P3HT/C₇₀–C₇₀ blends, as there is only one strong signal detectable (Figure 7). A closer look at this ESR spectrum reveals a shoulder at larger g factor (lower magnetic field). We have observed the underlying signal (shoulder) in several [70]fullerene-based blends, which is due to radical anions formed during the charge-transfer process.^[28] An example of such a C₇₀-related ESR

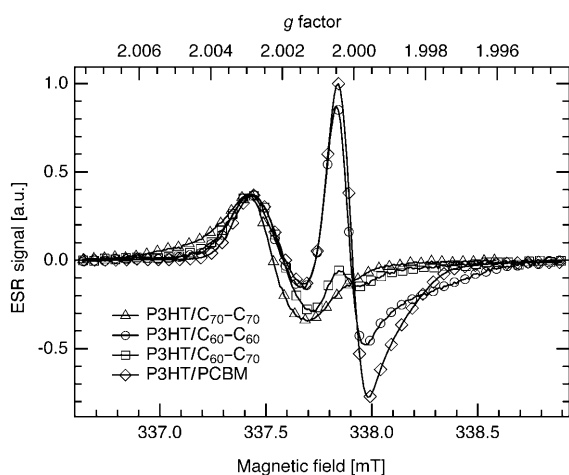


Figure 7. LESR signals in P3HT/fullerene blends at $T=120$ K. The curves are normalised to the $g=2.003$ peak of P3HT/[60]PCBM. Whereas the positive polaron on P3HT (low-field signal at $g=2.002$) is present in all blends, the negative polaron (high-field signals at $g=2.000$) is only seen in [60]PCBM or in C_{60} - C_{60} and C_{60} - C_{70} . At low magnetic field, a shoulder at $g=2.005$ due to the negative polaron on C_{70} - C_{70} can be seen in the P3HT/ C_{70} - C_{70} blends.

spectrum in P3HT blended with the commercial [70]PCBM is shown in the Supporting Information. We speculate, that this ESR signal is of the same origin as the 0.9 eV PIA peak found in the P3HT/ C_{70} - C_{70} PIA signals (Figure 6, inset), namely negative polarons on the C_{70} - C_{70} dimer.

From LESR measurements, it can be seen that the radical cation localised on the polymer backbone is not influenced by the choice of the acceptor molecule. In other words, all three compounds **4–6** act as acceptor when blended with P3HT. Also note that in compound **5**, radical anions (negative polarons) located on C_{60} and C_{70} cages can be observed simultaneously. This opens up a new interesting outlook of using fullerene heterodimers as model systems for studying spin–spin interactions.

Solar cell performance: The EQE and the current–voltage (J - V) characteristics were measured for all dimer blends. The EQE determines the number of generated charge carriers extracted into the outer circuit relative to the number of incident photons. Additionally, the short-circuit current density of the solar cell can be calculated for any illumination spectrum at a given intensity, in our case for the AM1.5G solar spectrum at 100 mW cm^{-2} . In J - V measurements, the intensity of the solar simulator used was adjusted to be equal to the calculated short-circuit current obtained from the EQE. This is an indirect method to accurately determine the main solar-cell parameters, such as short-circuit current density (J_{SC}), the open-circuit voltage (V_{OC}) and the fill factor (FF) of the solar cell.

Figure 8 shows the EQE spectra of BHJ solar cells with P3HT as electron donor and the three different dimers as acceptors. The EQE measurements yield values of 37, 31 and 25% for dimers **6**, **4** and **5**, respectively. The P3HT/dimer ratio was varied in a broad range of 4:1, 2.5:1, 2:1,

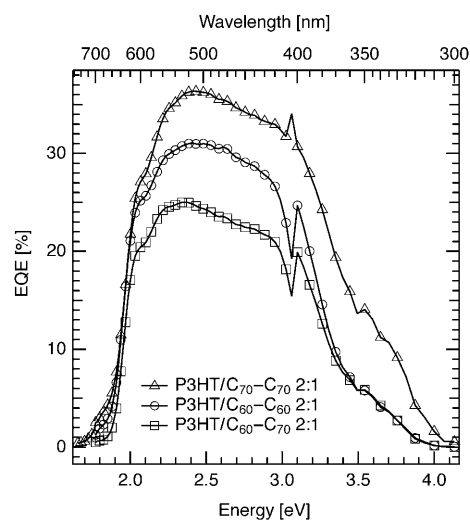


Figure 8. EQE of BHJ solar cells fabricated with P3HT blended with dimers **4–6** in 2:1 weight ratio.

1.5:1, 1:1, 1:2 and 1:4; however, the 2:1 blend ratio, that is, two parts of P3HT and one part of acceptor, was found to yield solar cells with the highest efficiencies. The corresponding J - V curves are shown in Figure 9. As can be seen,

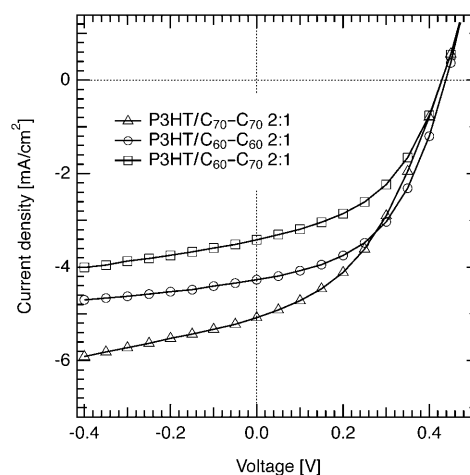


Figure 9. Current–voltage characteristics of P3HT/dimer BHJ solar cells at room temperature. $P=100 \text{ mW cm}^{-2}$.

the highest short-circuit current density of 5 mA cm^{-2} was achieved in P3HT/ C_{70} - C_{70} , the values being 4.3 and 3.4 mA cm^{-2} for P3HT/ C_{60} - C_{60} and P3HT/ C_{60} - C_{70} , respectively. Note that the heterodimer blends showed the smallest EQE and thus the smallest J_{SC} and PCE (Table 3).

Table 3. Characteristic parameters of the P3HT/dimer BHJ solar cell with weight ratio 2:1: the open-circuit voltage (V_{OC}), short-circuit current (J_{SC}), fill factor (FF) and calculated PCE.

	Ratio	V_{OC} [mV]	J_{SC} [mA cm^{-2}]	FF [%]	PCE [%]
	P3HT/ C_{60} - C_{60} 2:1	440	4.27	48	0.91
	P3HT/ C_{60} - C_{70} 2:1	430	3.41	46	0.67
	P3HT/ C_{70} - C_{70} 2:1	430	5.08	42	0.91

Conclusion

A new family of fullerene-based compounds, namely soluble [60]- and [70]fullerene homo- and heterodimers linked through 2-pyrazolino-pyrrolidino bridges, has been synthesised. Electrochemical, optical and ESR studies confirmed their suitability to act as electron acceptors in combination with regioregular P3HT. Compared to [60]PCBM, used in our work as a reference, the fullerene dimers exhibit a larger absorption coefficient thus justifying their use as absorber in BHJ solar cells. PL studies revealed that P3HT/ C_{70} - C_{70} blends show efficient PL quenching comparable to that of the P3HT/[60]PCBM system. The photogenerated polaron states in P3HT/ C_{70} - C_{70} blends have longer lifetimes than those of blends with [60]fullerene homo- and heterodimers, as follows from PIA experiments. The new PIA peak at 0.90 eV in P3HT/ C_{70} - C_{70} blends was identified and suggested to result from a radical anion. LESR studies on all blends confirmed this finding, as a radical anion could solely be identified in C_{70} - C_{70} dimer-based blends. The P3HT/ C_{60} - C_{70} blend instead displayed a reduced PL quenching, thus indicating inefficient charge transfer. This blend shows a shoulder at 1.03 eV in the PIA spectrum, which is due to unquenched excitons in the blend. We tentatively assign the 1.03 eV PIA peak to charge-transfer exciton states; however, triplet excitons could also be responsible. According to our expectations, the P3HT/ C_{70} - C_{70} blends should be most promising for BHJ solar cells. Our preliminary tests demonstrated the non-optimised PCE of about 1% in ITO/PEDOT/PSS/P3HT/ C_{70} - C_{70} /Al PV devices (see Experimental Section). The P3HT/ C_{70} - C_{70} -based solar cells exhibited the most promising EQEs and PCEs, which were as high as 37 and 0.91%, respectively. The solar cells are by no means optimised and with a view to obtaining competitive PCEs, the morphology of the blends should be thoroughly investigated.

Experimental Section

Sample preparation for optical and ESR spectroscopy: UV/Vis spectra were obtained in both toluene solutions (at 1×10^{-5} M) and in solid films. PIA measurements were performed on thin films of pure P3HT and P3HT blended with fullerene dimers. Regioregular P3HT was purchased from Rieke Metals and used without further purification. As a reference acceptor in BHJs, we used PCBM purchased from Solenne BV. All materials were dissolved in dichlorobenzene at a concentration of 10 mg mL⁻¹. The films were deposited onto sapphire substrates by spin-coating and annealed at 120 °C for 10 min. If not stated otherwise, blends with a 1:1 weight ratio were studied. Films were prepared under a nitrogen atmosphere in a glove box to prevent ageing effects due to water and oxygen. The samples for ESR were drop-cast on a flexible substrate, wrapped up and placed in a sealed quartz tube (Wilmad-LabGlass) in the centre of a microwave cavity.

Electrochemistry: The electrochemical properties of dimers 4–6 and the precursor aldehydes 7 and 9 (Schemes 1 and 2) were studied at room temperature by CV and OSWV in ODCB/CH₃CN (4:1) as solvent, with Bu₄N⁺PF₆⁻ as the supporting electrolyte.

Optical absorption and photoluminescence: UV/Vis absorption spectra were recorded with a Perkin-Elmer Lambda 900 spectrometer at room

temperature. PL measurements were performed with the same set-up as that used for PIA.

Photoinduced absorption: For PIA measurements, the samples were mounted on a helium cold-finger cryostat (20–293 K) and kept under dynamic vacuum to avoid photo-oxidation. The excitation source was a mechanically chopped argon-ion laser (Melles Griot) at a wavelength 514 nm with a power of 68 mW. Additionally, a halogen lamp provided continuous-wave illumination. Both light sources were focussed onto the same point of the sample. The transmitted light was collected by large-diameter concave mirrors and focussed into the entrance slit of a cornerstone monochromator. Depending on the wavelength, detection was provided by a silicon diode (550–1030 nm) or by a liquid-nitrogen-cooled InSb detector (1030–5550 nm). Therefore, a broad energy range of 0.23–2.25 eV (with KBr cryostat windows) was accessible. The signals were recorded with a standard phase-sensitive technique synchronised with the chopping frequency of the laser by using a signal recovery 7265 DSP lock-in amplifier. Photoinduced changes of the transmission, $\Delta T/T$, were monitored as function of the wavelength of the probe light. Frequency-resolved PIA measurements were carried out by varying the frequency of the chopper of the argon-ion laser, $\omega/2\pi$, between 56 and 20 000 Hz. The lifetimes of the long-lived (about ms– μ s) excitations were deduced by fitting the $\Delta T/T(\omega)$ dependence.

Electron spin resonance: To verify the presence of the spin-carrying polarons in the polymer–fullerene films after photoexcitation, we used the ESR technique (Bruker ESR200D). A 150 W halogen lamp guided to the microwave cavity was used for excitation. All measurements presented here were performed at 120 K by cooling with a liquid nitrogen flow. A static magnetic field of 0.33 T was superimposed with the ac magnetic field at $f=100$ kHz modulation frequency, which allowed phase-sensitive lock-in detection. By using the first derivative of the Voigt line shape, the overlapping ESR signals from negative and positive polarons (radical anions and radical cations) were deconvoluted. The g factor of the ESR signals was calibrated for every measurement with a Bruker 035M NMR gaussmeter and an EIP 28b frequency counter.

Preparation of PV devices: BHJ solar cells were processed by spin-coating a mixture of P3HT and the fullerene dimers on an oxygen-plasma-treated indium tin oxide (ITO)-coated glass substrate, coated with a 40 nm layer of poly(3,4-ethylenedioxythiophene)/poly(styrenesulfonate) (PEDOT/PSS). The PEDOT/PSS layer was treated at 180 °C for 10 min and then transferred to a nitrogen glove box. P3HT and dimers were dissolved in ODCB (20 mg mL⁻¹) and blended in various donor-to-acceptor ratios. The weight ratio was varied in the range from 4:1 to 1:4 for each of the three dimers. The blend solution was then spin-coated onto the substrates at 800 rpm for 240 s, which resulted in a layer of thickness 110 nm. The film thickness was measured by a Dektak surface profiler (Veeco). Before evaporating the 80 nm thick Al cathode, all samples were thermally treated at 120 °C for another 10 min. As a reference acceptor in BHJs, we used PCBM purchased from Solenne BV.

PV characterisation: Current–voltage measurements were recorded with a Keithley 237 SMU instrument. A 300 W xenon lamp was used for illumination. Monochromatic EQE spectra were obtained with a homemade lock-in set-up equipped with a calibrated photodiode. The light from the halogen and xenon lamps was spectrally dispersed by a monochromator with a set of gratings to cover the wavelength region from 250 to 1000 nm. Although the mismatch factor of the xenon lamp to the AM1.5 spectrum was not determined, we used an indirect method to determine the PCE accurately. The short-circuit current density of the solar cell was calculated from the EQE for an AM1.5 spectrum at a given light intensity, for example 1000 W m⁻², and the solar simulator in the current–voltage measurements was then adjusted to obtain the short-circuit current from the solar cell under test.

Acknowledgements

This work was supported by the MEC of Spain (Ramón y Cajal Program and projects CTQ2008-00795/BQU and Consolider-Ingenio 2010C-07-

25200), the CAM (project P-PPQ-000225-0505), the ESF (project 05-SONS-FP-021) and the DFG SPP project "Elementary processes in organic photovoltaics", under contract DY18/6-1. V.D.'s work at the ZAE Bayern is financed by the Bavarian Ministry of Economic Affairs, Infrastructure, Transport and Technology. We also thank Andreas Baumann and Daniel Rauh (University of Würzburg) for the photovoltaic studies.

- [1] P. Friedlingstein, *Nature* **2008**, *451*, 297.
 [2] J. Potocnik, *Science* **2007**, *315*, 810.
 [3] a) M. A. Green, K. Emery, Y. Hishikawa, W. Warta, *Prog. Photovoltaics* **2009**, *17*, 85; b) I.-W. Hwang, D. Moses, A. J. Heeger, *J. Phys. Chem. C* **2008**, *112*, 4350.
 [4] a) B. C. Thompson, J. M. J. Fréchet, *Angew. Chem.* **2008**, *120*, 62; *Angew. Chem. Int. Ed.* **2008**, *47*, 58; b) S. Günes, H. Neugebauer, N. S. Sariciftci, *Chem. Rev.* **2007**, *107*(4), 1324.
 [5] a) *The Chemistry of Fullerenes* (Ed.: A. Hirsch), Wiley-VCH, Weinheim, **2005**; b) *Fullerenes: From Synthesis to Optoelectronic Properties* (Eds.: D. M. Guldi, N. Martín), Kluwer Academic Publishers, Dordrecht, **2002**; c) *Lecture Notes on Fullerene Chemistry: A Handbook for Chemists* (Ed.: R. Taylor), Imperial College Press, London, **1999**; d) *Fullerenes: Principles and Applications* (Eds.: F. Langa, J.-F. Nierengarten), RSC, Cambridge, **2007**; e) N. Martín, *Chem. Commun.* **2006**, 2093.
 [6] a) M. Svensson, F. Zhang, S. C. Veenstra, W. J. H. Verhees, J. C. Hummelen, J. M. Kroon, O. Inganäs, M. R. Andersson, *Adv. Mater.* **2003**, *15*, 988; b) F. Zhang, K. G. Jespersen, C. Björström, M. Svensson, M. R. Andersson, V. Sundström, K. Magnusson, E. Moons, A. Yartsev, O. Inganäs, *Adv. Funct. Mater.* **2006**, *16*, 667.
 [7] X. Wang, E. Perzon, J. L. Delgado, P. de la Cruz, F. Zhang, F. Langa, M. Andersson, O. Inganäs, *Appl. Phys. Lett.* **2004**, *85*, 5081.
 [8] J. C. Hummelen, B. W. Knight, F. LePeq, F. Wudl, J. Yao, C. L. Wilkins, *J. Org. Chem.* **1995**, *60*, 532.
 [9] a) W. Ma, C. Yang, X. Gong, K. Lee, A. J. Heeger, *Adv. Funct. Mater.* **2005**, *15*, 1617; b) G. Li, V. Shrotriya, J. Huang, Y. Yao, T. Moriarty, K. Emery, Y. Yang, *Nat. Mater.* **2005**, *4*, 864.
 [10] I. Riedel, E. von Hauff, J. Parisi, N. Martin, F. Giacalone, V. Dyakonov, *Adv. Funct. Mater.* **2005**, *15*, 1979.
 [11] S. Backer, K. Sivula, D. F. Kavulak, J. M. J. Fréchet, *Chem. Mater.* **2007**, *19*, 2927.
 [12] a) M. M. Mandoc, F. B. Kooistra, J. C. Hummelen, B. de Boer, P. W. M. Blom, *Appl. Phys. Lett.* **2007**, *91*, 263505; b) F. B. Kooistra, J. Knol, J. Kastenberg, L. M. Popescu, W. J. H. Verhees, J. M. Kroon, J. C. Hummelen, *Org. Lett.* **2007**, *9*, 551.
 [13] M. M. Wienk, J. M. Kroon, W. J. H. Verhees, J. Knol, J. C. Hummelen, P. A. van Hal, R. A. J. Janssen, *Angew. Chem.* **2003**, *115*, 3493; *Angew. Chem. Int. Ed.* **2003**, *42*, 3371.
 [14] For a review on fullerene dimers, see: a) J. L. Segura, N. Martín, *Chem. Soc. Rev.* **2000**, *29*, 13; b) J. L. Segura, E. M. Priego, N. Martín, C. P. Luo, D. M. Guldi, *Org. Lett.* **2000**, *2*, 4021; c) J. J. González, S. González, E. M. Priego, C. P. Luo, D. M. Guldi, J. de Mendoza, N. Martín, *Chem. Commun.* **2001**, 163–164.
 [15] a) J. L. Delgado, F. Cardinali, E. Espíldora, M. R. Torres, F. Langa, N. Martín, *Org. Lett.* **2008**, *10*, 3705; b) J. L. Delgado, F. Oswald, F. Cardinali, F. Langa, N. Martín, *J. Org. Chem.* **2008**, *73*(8), 3184.
 [16] C. Thilgen, A. Herrmann, F. Diederich, *Angew. Chem.* **1997**, *109*, 2362; *Angew. Chem. Int. Ed. Engl.* **1997**, *36*, 2268.
 [17] S. R. Wilson, Q. Lu, *J. Org. Chem.* **1995**, *60*, 6496.
 [18] a) T. J. Hingston, M. R. Sambrook, N. H. Rees, K. Porfirakis, G. Andrew, D. Briggs, *Tetrahedron Lett.* **2006**, *47*, 8595; b) J.-F. Nierengarten, A. Herrmann, R. R. Tykwinski, M. Riittimann, F. Diederich, C. Boudon, J.-P. Gisselbrecht, M. Gross, *Helv. Chim. Acta* **1997**, *80*, 293.
 [19] a) K. Komatsu, K. Fujiwara, Y. Murata, *Chem. Commun.* **2000**, 1583; b) H.-J. Eisler, F. H. Hennrich, E. Werner, A. Hertwig, C. Stoermer, M. M. Kappes, *J. Phys. Chem. A* **1998**, *102*, 3889.
 [20] F. Oswald, M. E. El-Khouly, Y. Araky, O. Ito, F. Langa, *J. Phys. Chem. B* **2007**, *111*, 4335.
 [21] a) M. Maggini, G. Scorrano, M. Prato, *J. Am. Chem. Soc.* **1993**, *115*, 9798; b) M. Prato, M. Maggini, *Acc. Chem. Res.* **1998**, *31*, 519; c) N. Tagmatarchis, M. Prato, *Synlett* **2003**, 768.
 [22] The assignment of the three isomers was performed by taking into consideration the Supporting Information included in ref. [20], in which isomers of compound **8** were characterized.
 [23] a) S. Muthu, R. Maruthamuthu, P. R. Ragunathan, P. R. Vasudeva, C. K. Rao, *Tetrahedron Lett.* **1994**, *35*, 1763; b) Y. Matsubara, H. Tada, S. Nagase, Z. Yoshida, *J. Org. Chem.* **1995**, *60*, 5372; c) F. Langa, F. Oswald, *C. R. Chim.* **2006**, *9*, 1058; d) J. L. Delgado, P. de la Cruz, V. López-Arza, F. Langa, *Tetrahedron Lett.* **2004**, *45*, 1651; e) F. Langa, P. de la Cruz, E. Espíldora, A. de la Hoz, J. L. Bourdelande, L. Sanchez, N. Martín, *J. Org. Chem.* **2001**, *66*, 5033.
 [24] a) N. Martín, L. Sanchez, B. Illescas, I. Perez, *Chem. Rev.* **1998**, *98*, 2527; b) L. Echegoyen, L. E. Echegoyen, *Acc. Chem. Res.* **1998**, *31*, 593.
 [25] a) Z. Vardeny, E. Ehrenfreund, O. Brafman, M. Novak, H. Schaffer, A. J. Heeger, F. Wudl, *Phys. Rev. Lett.* **1986**, *56*, 671; b) P. Lane, X. Wei, Z. Vardeny, *Phys. Rev. B* **1996**, *77*, 1544.
 [26] R. Österbacka, C. P. An, X. M. Jiang, Z. V. Vardeny, *Science* **2000**, *287*, 839.
 [27] O. Epshtein, G. Nakhmanovich, Y. Eichen, E. Ehrenfreund, *Phys. Rev. B* **2001**, *63*, 125206.
 [28] O. Poluektov, S. Filippone, N. Martin, A. Sperlich, C. Deibel, V. Dyakonov, unpublished results.

Received: July 22, 2009
Published online: November 5, 2009